Jurnal Agronomi Indonesia
(Indonesian Journal of Agronomy)

ISSN 2085-2916 | e-ISSN 2337-3652
April 2024, *52*(1), 29-37
DOI: https://dx.doi.org/10.24831/jai.v52i1.50770

Research Article

Application of RGB UAV images to identify spectral patterns and estimate rice production

Khursatul Munibah [1,*], Wahyu Iskandar [1,2], Baba Barus [1,2], and Chiharu Hongo [3]

[1] Department of Soil Science and Land Resource, Faculty of Agriculture, IPB University (Bogor Agricultural University), Jl. Meranti, Kampus IPB Dramaga, Bogor 16680, INDONESIA
[2] Center for Regional System Analysis, Planning, and Development (CRESPENT), IPB University (Bogor Agricultural University), Jl. Pajajaran, Kampus IPB Baranangsiang 16127, INDONESIA
[3] Center for Environmental Remote Sensing (CERES), Chiba University, JAPAN
* Corresponding author (✉ munibah@apps.ipb.ac.id)

ABSTRACT

Monitoring rice plant growth is crucial for evaluating rice field management and yield production. RGB images are generated from Unmanned Aerial Vehicles (UAV) with RGB cameras. UAVs produce high spatial and temporal resolution, while RGB cameras are commonly used and cheap. The objectives of this study were to identify the spectral pattern of rice plant growth and to estimate yield production based on the spectral value of RGB images. The spectral pattern and yield estimation were analyzed using confidence interval (CI) and regression, respectively. Results show that spectral pattern during the vegetative until ripening stage forms a concave with minimum value in the generative stage and decreases towards the harvest stage. Based on the CI value, the high interval between upper and lower happened in the vegetative and ripening stages while the low interval happened in the generative stage. The high CI in the vegetative and ripening stages was due to the soil background and complexity of the rice plant canopy, respectively while the low CI in the generative stage was due to the homogeneous response of the leaf canopy. The best rice yield estimation based on the spectral value occurs in the ripening stage with an R^2 of 0.84.

Keywords: chlorophyll content, confidence interval, drone images, rice plant, regression

Edited by:
Okti Syah Isyani Permatasari
IPB University

Received:
12 October 2023
Accepted:
14 March 2024
Published online:
6 May 2024

Citation:
Munibah, K., Iskandar, W., Barus, B., Hongo, C. (2024). Application of RGB UAV images to identify spectral patterns and estimate yield of rice field. *Jurnal Agronomi Indonesia (Indonesian Journal of Agronomy)*, *52*(1), 29-37

INTRODUCTION

Despite being awarded by IRRI for "Acknowledgment for Achieving Agri-food System Resiliency and Rice Self-Sufficiency during 2019-2021 through the Application of Rice Innovation Technology", rice production is still a major concern in Indonesia. Rice production is challenged by a continuously growing population, land-use changes, and limited access to innovation, technologies, and resources (Sujarwo et al., 2022). A huge work is necessary to achieve the rice availability target of 46,84 million tons in 2024. Rice production in 2015–2022 was stagnant and tended to decrease by 0.21% per year (Santosa, 2023). Also, rice self-sufficiency still needs to be maintained for a long time.

To secure rice productivity, early monitoring is important to identify the crop condition, to improve rice crop management, and eventually to estimate rice production (Sari et al., 2021). Rice plant characteristics that can be monitored are plant height (Muangprakhon & Kaewplang, 2021), chlorophyll content index (Ban et al., 2022; Wang et al., 2023), number of tillers (Munibah et al., 2022) and leaf area index (LAI) (Gong et al., 2021). Those characteristics are important to understand the crop condition. Leaf chlorophyll can absorb strongly in the blue (about 430 nm) and the red (about 660 nm) light but most of the green light is reflected into human eyes so the leaves appear green

(Taiz & Zeiger, 2002). The absorbed light will support the photosynthesis process to produce carbohydrates which will be the rice grain. So leaf chlorophyll has an important role in plant growth which is followed by changes in plant characteristics, such as an increase in plant height, number of tillers, and LAI. Growth-associated characteristics of plants, such as chlorophyll content and water content, can be quantified using remote-sensing instruments (Chapman et al., 2014). Leaf chlorophyll and plant photosynthesis are strongly correlated, as plants with higher chlorophyll have a greater photosynthetic capacity and accumulate more photosynthetic products (Wang et al., 2023).

Increasing rice production is the main goal of various studies on paddy fields. Estimation of rice yield is one way to evaluate and improve rice field management to achieve the main goal. For planners, government, and decision-makers, the rice field estimation is a good stape for formulating policies regarding import/export in the event of shortfall and/or surplus (Nazir et al., 2021). Optimum agronomic management of rice plants during the first weeks of rice cultivation (40-50 days after planting) and three months before the harvest, farmers can improve their management practices to achieve high yields (Franch et al., 2021). Remote sensing data is data that is often used to estimate rice yields, such as Landsat (Siyal et al., 2015), Sentinel-2 (Franch et al., 2021), and UAV (Duan et al., 2019; Bascon et al., 2022) owing to the close correlation between the rice yield and the spectral information from satellite imagery (Franch et al., 2021). The best estimation model of Wheat yield using Sentinel-2 time series and Multiple Linear Regression (MLR) techniques is the Green Normalized Difference Vegetation Index (GNDVI) in the tillering (R^2=0.9) and maturity stages (R^2=0.71) (Imanni et al., 2022).

Remote sensing is the science and art of obtaining information about an object, area, or phenomenon through the analysis of data acquired by a device that is not in contact with the object, area, or phenomenon under investigation (Lillesand et al., 2014). Unmanned Aerial Vehicle (UAV) is one remote sensing platform to collect data and monitor crop conditions with high spatiotemporal resolution imagery (Duan et al., 2019; Sari et al., 2021; Bascon et al., 2022). UAVs have abilities to acquire the earth's surface with low flight (more detail) and short revisit time on the same location (more database). The development of UAV, low altitude remote sensing technology has been applied in monitoring pests and diseases on rice canopy because of UAV's high automation and flexibility (Li et al., 2022). In comparison to satellite remote sensing, the spatial and temporal resolution of UAVs can be adjusted flexibly according to the requirements (Du et al., 2022). The UAVs with RGB cameras have received increasing attention due to their high spatial and temporal resolution and relatively low cost (Du et al., 2022). The detailed data generated by the RGB UAV can be used to validate remote sensing data like Landsat 8 or Sentinel-2. However, the measurements are taken on the same day of the satellite passage, and a maximum time interval of ±3 hours to capture the image (Ariza et al., 2018) or depending on the subject being investigated has not changed. Hence, the purpose of the research is (i) to identify the spectral pattern of the rice field based on the spectral of RGB UAV images, and (ii) to estimate the rice yield based on the spectral of RGB UAV images.

MATERIALS AND METHODS

Study area

The study site was irrigated rice fields (blocks 7B and 4B) situated in Bojongpicung Subdistrict, Cianjur Regency, West Java (Figure 1). The rice fields (Inpari 32 variety) were managed by the Ministry of Agriculture.

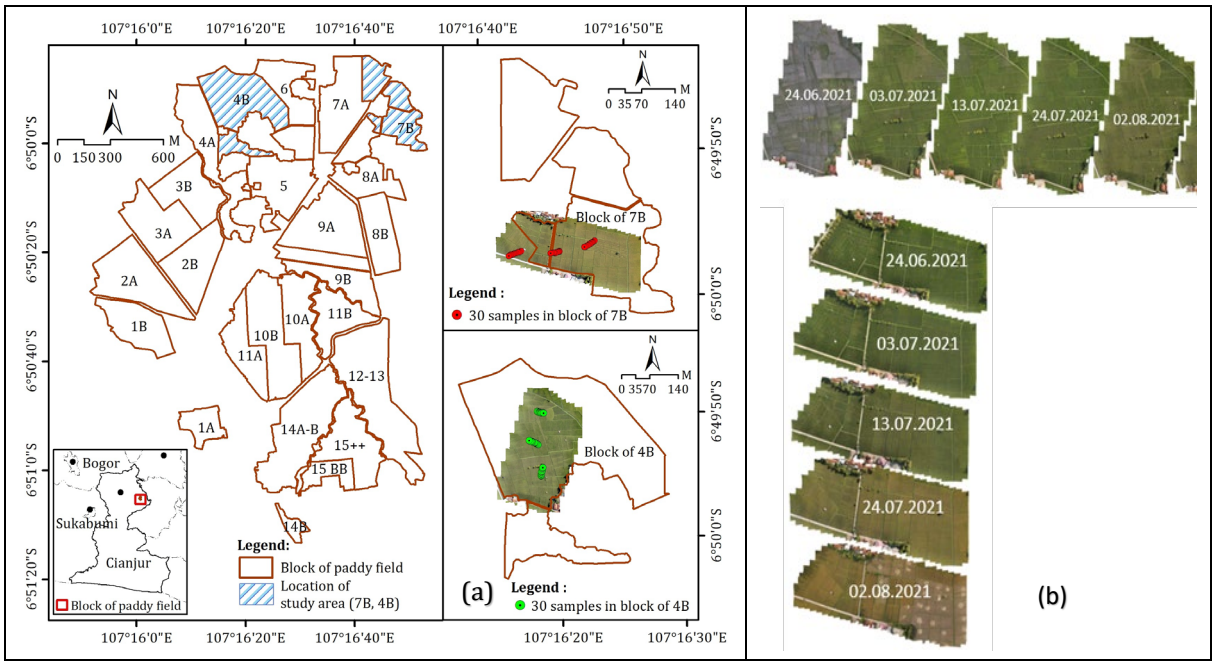

Figure 1. Study area (a) and mosaics of RGB UAV images (b) in Bojongpicung Subdistrict, Cianjur Regency, West Java.

Data collection

The temporal RGB UAV images as primary data were collected during a single rice growth cycle of 7B (09 May-05 August 2021) and 4B (09 May-15 August 2021). However, RGB UAV acquisitions were undertaken around 09.00-11.00 AM at 10-day intervals (on 24 June; 04 July; 13 July; 24 July, and 02 August 2021). The number of UAV images for each block ranges from 454-775 sheets and the mosaics are presented in Figure 1b. The altitude for data acquisition of RGB UAV images was 50 m from the ground surface equivalent to 2.64 cm (spatial resolution).

Ten sample locations for each block (4B and 7B) were distributed diagonally in each block (Figure 2). The distribution of sample data at each UAV acquisition date and growth stage is presented in Table 1. Classification of the growth stage of rice plants based on International Rice Research Institute (IRRI) and modification based on the variety of Inpari 32, namely (a) wet fallow (-20-0 DAP), (b) vegetative (1-35 DAP), (c) generative (36-65 DAP), (d) ripening (66-86 DAP), (e) harvesting (86-100 DAP), (f) dry fallow (101-130 DAP).

Table 1. Date and rice stage of sampling data.

Plant age (Days after planting)	Acquisition date (2021)					Number of sample data
	24 June	04 July	13 July	24 July	02 August	
26 days (vegetative)	10	0	0	0	0	10
36 days (vegetative)	20	10	0	0	0	30
46 days (generative)	30	20	10	0	0	60
56 days (generative)	0	30	20	10	0	60
66 days (generative)	0	0	30	20	10	60
76 days (ripening)	0	0	0	30	20	50
86 days (ripening)	0	0	0	0	30	30
Total	60	60	60	60	60	300

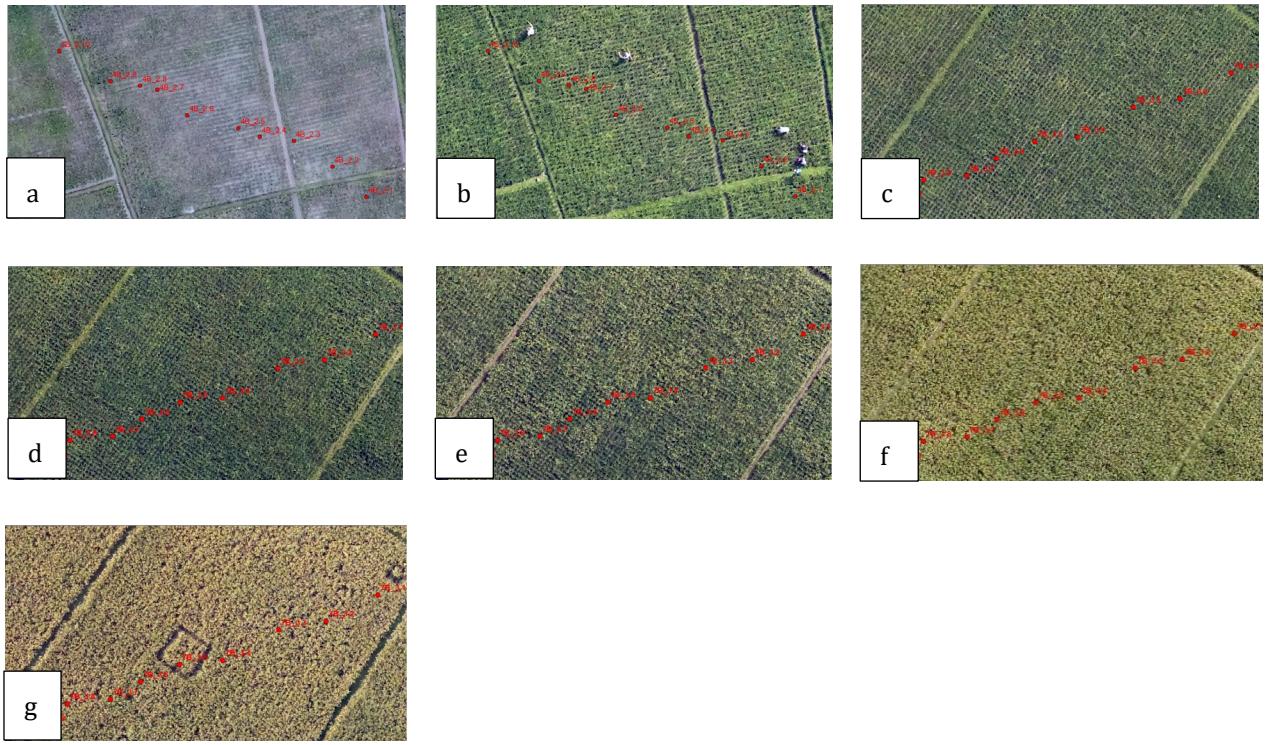

Figure 2. Rice field performance on RGB UAV with sample point (red color): (a) at 4B. age 26 DAP, (b) at 4B. age 36 DAP, (c) at 7B. age 46 DAP, (d) at 7B. age 56 DAP, (e) at 7B. age 66 DAP, (f) at 7B. age 76 DAP, (g) at 7B. age 86 DAP.

Data analysis

All RGB UAV images were mosaicked according to the acquisition time using Agisoft Metashape, Version 2.0 (Agisoft, 2022). The spectral value of rice fields was represented by a digital number (DN) from RGB UAV with a range of 0 to 255 (8-bit). The spectral pattern of rice fields in RGB UAV images was analyzed based on values mean, standard deviation, and confidence interval (CI) with a 95% confidence level. The CI is possible to use a sample statistic and estimates of error in the sample to get a fair idea of the population parameter, not as a single value, but as a range of values (Hazra, 2017).

The estimation of rice yield was based on the spectra of RGB UAV. The estimation of rice yield was analyzed using a linear regression, where dependent and independent variables were the rice yield and the spectral value, respectively.

RESULTS AND DISCUSSION

UAV spectral pattern of rice field in various stages of growth

Figure 3a shows that the RGB UAV spectral of a rice field during one cycle of growth between vegetative and ripening formed a concave with a minimum value at the generative stage and decreased towards the harvest stage. The spectral value of RGB light in the vegetative stage (26 DAP) was high and similar. White to gray appeared which was possibly an effect of fertilizer application at 26 DAP. This fertilizer application suggested a higher spectral value of RGB light compared to normal conditions. During fertilizer application, the rice field was covered by stagnant water containing fertilizer (Figure 4a). However, in a couple of days irrigating water was stopped implying that fertilizer was deposited in the soils (Figure 4b). Eventually, aquatic weeds like *Kayambang/Apu-apu* (*Pistia stratiotes*) grew in between the rice plants (Figure 4c).

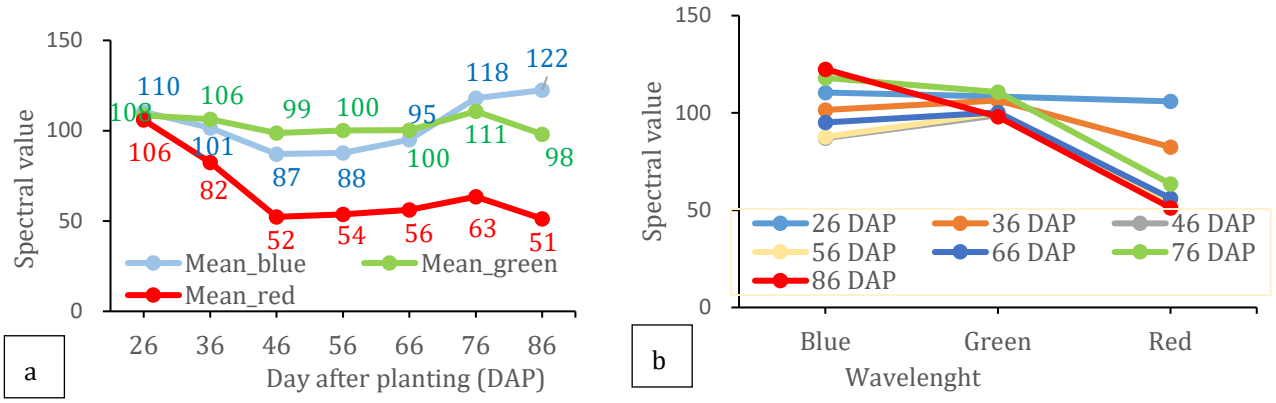

Figure 3. Relationship between the mean of the RGB UAV spectral of rice field with (a) age and (b) wavelength.

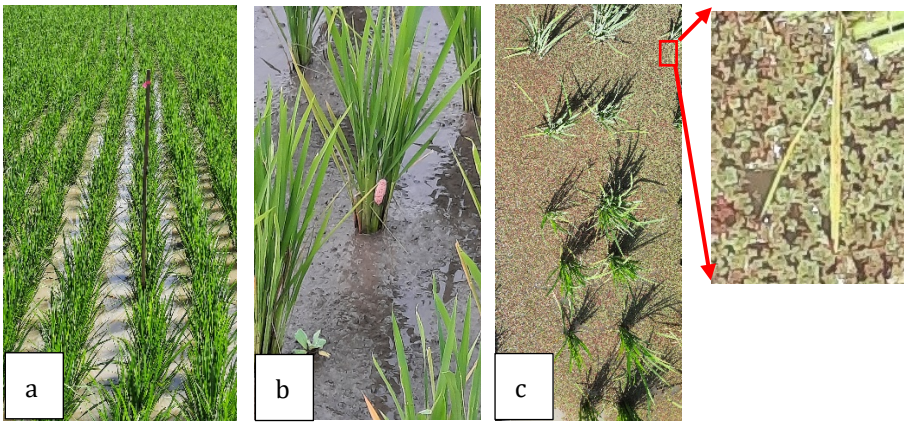

Figure 4. The stagnant water condition during fertilizer application (a), fertilizer deposits (b), and aquatic weed (c) on the rice field under fertilization condition.

In the concave pattern of RGB spectral values in our study, the maximum absorbance of blue and red bands occurred during the generative stage. The pattern confirms previous reports that rice leaves in the vegetative stage absorbed visible (RGB) light (Gong et al., 2021) until they reached maximum absorption in the generative stage due to the development of leaf growth (Taiz & Zeiger, 2002). During the ripening to harvest stage, the absorption of visible (RGB) light by the leaf decreases (Figure 3a) because leaf development (high chlorophyll) is replaced by panicle development (low chlorophyll). The absorption of panicle is lower than leaf or in other word the reflectance of panicle is higher than leaf.

Figure 3b shows that the age of rice plants could be distinguished in the blue band of RGB UAV images even by small differences in spectral values. In the green band, the age of rice plants is difficult to distinguish for all ages because green light is less sensitive to differences in chlorophyll content. In the red band, rice plants aged 26 DAP, 36 DAP, 78 DAP, and 86 DAP can be distinguished more easily than those in the blue or green band. This is because the difference in spectral values between plant ages in the red band was greater than in the blue or green bands. Although the use of RGB wavelengths such as in Sentinel-2A is not as good as near-infrared (NIR) in its ability to distinguish the age of rice plants (Kawamura et al., 2018; Munibah et al., 2019; Hisham et al., 2022). Our result shows that RGB UAV was reliable in distinguishing the spectral value pattern in a single rice cycle. Hence, we suggest that the use of RGB UAV is promising to assist in monitoring rice plant condition, growth, and stage with more flexibility in spatial and temporal resolution.

Confidence interval (CI) value of rice field spectral in various stages of growth

Figure 5 shows the distribution of a sample of RGB UAV spectra in various stages of rice plant growth with upper and lower bounds at 95% CI. Based on the CI value, on the blue band (Figure 5a) where the difference between upper and lower CI in the vegetative stage (26 DAP) is 10.42 with CI (105.15; 115.68) and tends to decrease to minimum interval in the generative stage (56 DAP) of 8.08 with CI (83.63; 91.71) and increases to 13.22 with CI (113.08; 131.77) in ripening stage (86 DAP). On the green band (Figure 5b) where difference between upper and lower CI in the vegetative stage (26 DAP) is 9.04 with CI (103.94;112.98) and tends to decrease to the minimum interval in the generative stage (56 DAP) of 8.47 with CI (95.82;104.29) and increases to 18.14 with CI (89.03; 107.17) in ripening stage (86 DAP). On the red band (Figure 5c) where difference between upper and lower CI in the vegetative stage (26 DAP) is 13.40 with CI (99.23;112.63) and decreases to the minimum interval in the generative stage (56 DAP) of 5.79 with CI (56.67;50.89) and increases to 13.22 with CI (57.84;44.62) in ripening stage (86 DAP). There are two samples (1 and 2) each found in RGB UAV images which were respectively acquired on 24 June 2021 and 04 July 2021 (Figures 5a, 5b, and 5c). Spectral values of the two samples are far from the values in the box plot which are known as outlier values. Object 1 and object 2 are the rice fields covered by other bright objects that have high spectral values.

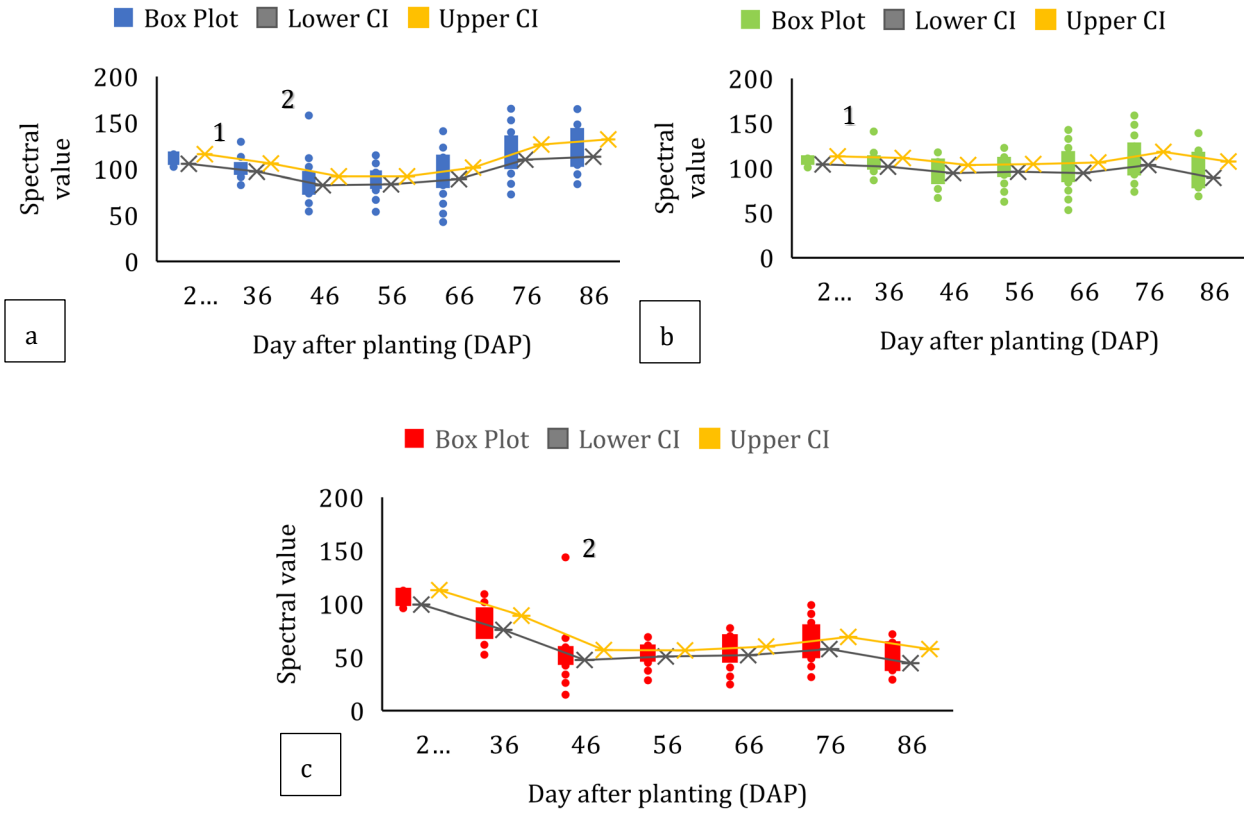

Figure 5. Confidence interval (CI) of rice field spectral in blue band (a), green band (b), and red band (c) on various stages of growth.

Figure 6 shows the dynamics of value changes between the upper and lower of the CI value, where the vegetative stage is wider because of the soil background. Conditions in the field showed that the leaf canopy density of rice plants (especially 26 DAP) was still low and paddy fields were dominated by standing water mixed with fertilizer, fertilizer deposits, and water weeds during the fertilization period. In the generative stage, the interval between upper and lower was smaller and even reached a minimum interval in rice plants at 56 DAP. This is because the canopy coverage was dense enough to cover the ground that was composed of green leaves and young panicles with green color. In the ripening stage, the interval between the upper and lower CI was even wider because of

the complexity of the canopy covering the ground. A complex rice plant canopy is a canopy that is composed of many features, such as green leaves, brownish green, brown, and mature panicles which are brown.

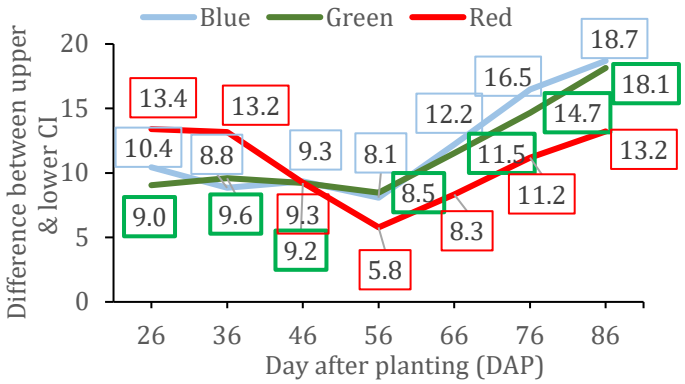

Figure 6. The dynamics of values change between upper and lower confidence intervals

Estimation of rice yield based on RGB UAV spectral on various stages of growth

Figure 7a shows that the best rice yield estimation model based on the RGB UAV spectral occurs in rice plants on the ripening stage (86 DAP) with R^2 of 0.84. The result suggests that the RGB UAV spectral could explain 84% of the estimation model of rice yields, the rest is influenced by other factors. The rice field at age 86 DAP was dominated by the rice grain and brown leaves because of the very low chlorophyll content (Figure 7b). The high correlation at reproductive phases could be associated with the formation productive stage (panicle, heading/booting, flowering) and ripening stage (milk, dough, and maturity of grain), which directly influence the crop yields (Nazir et al., 2021; Kawamura et al., 2018). The result of this study is also consistent with the findings of existing literature, where the ripening stage highly influences rice yield production. Another study produced slightly different from this study but it is still consistent with the findings of existing literature because different in terms of methodology. The NDVI of the Sentinel-2 image performs the best yield on the booting stage and highly influences the rice yield production (high R^2 of 0.83 and low RMSE of 0.12 tons ha^{-1}) (Nazir et al., 2021). The booting stage might be the best time for in-season rice grain assessment based on hyperspectral sensing data with R^2=0.843 (Kawamura et al., 2018). The booting stage represents the peak period of nutrient growth for rice plants which can be attributed to the maximal photosynthetic capacity and yield potential (Kawamura et al., 2018). Thus, the growth of rice plants in the reproductive and ripening stages should be classified into more detailed growth phases when it is related to production.

In this study, the rice plant in the early reproductive stage (46 DAP), late reproductive stage (66 DAP), and ripening stage (76 DAP) are not good enough to be used for estimating rice yields because of low R^2 value, while rice plant on middle reproductive stage (56 DAP) is better with R^2=0.54. This means the model of RGB UAV reflectance can explain only 54% of rice yields, the rest is influenced by other factors. The ability of leaves to photosynthesize increases at the beginning of leaf development and then decreases after maximum leaf development (Taiz & Zeiger, 2002). Rice plants (variety Inpari 32) aged 56 days after planting are in a transition between late vegetative and early generative where leaf development reaches its peak and panicle formation begins. This transition period provides an estimated model of results based on RGB UAV spectral with R^2=54%.

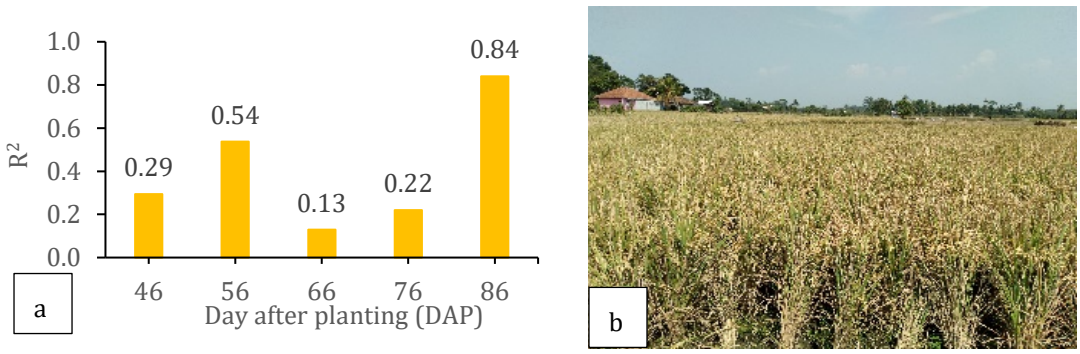

Figure 7. Determination coefficient (R^2) of estimation model of yield rice based on spectral (a) and (b) rice field at 86 DAP.

CONCLUSIONS

RGB UAV images of rice plants have a concave pattern starting from the vegetative to the ripening stage and decreasing towards the harvest stage. RGB UAV images can be used to distinguish the age of rice plants in the blue and red bands. The heterogeneity of response of rice fields is indicated by the high range of confidence interval (CI) values between upper and lower due to variations in soil background and canopy of rice fields. The best estimation of rice yield based on the reflectance occurs in the ripening stage (86 DAP) with R^2 =0.84.

ACKNOWLEDGEMENTS

The authors would like to acknowledge funding support from IPB University through the Agromaritime Program and also the devices support from Chiba University through SATREPS (Science and Technology Research Partnership for Sustainable Development) activities. We thank our colleagues in the Division of Remote Sensing and Spatial Information, Department of Soil Science and Land Resources for their kind support during manuscript preparation.

REFERENCES

Agisoft. (2022). *Agisoft Metashape User Manual: Professional Edition, version 1.8*. Agisoft LLC.

Ariza, A., Irizar, M. R., & Bayer, S. (2018). Empirical line model for the atmospheric correction of sentinel-2A MSI images in the Caribbean Islands. *European Journal of Remote Sensing*, *51*(1), 765–776. https://doi.org/10.1080/22797254.2018.1482732

Hisham, N. H. B., Hashim, N., Saraf, N. M., & Talib, N. (2022). Monitoring of rice growth phases using multi-temporal sentinel-2 satellite image. *IOP Conference Series: Earth and Environmental Science*, *1051*, 1–13. https://doi.org/10.1088/1755-1315/1051/1/012021

Ban, S., Liu, W., Tian, M., Wang, Q., Yuan, T., Chang, Q., & Li, L. (2022). Rice leaf chlorophyll content estimation using UAV-based spectral images in different regions. *Agronomy*, *12*(11), 2832. https://doi.org/10.3390/agronomy12112832

Bascon, M. V., Nakata, T., Shibata, S., Takata, I., Kobayashi, N., Kato, Y., Inoue, S., Doi, K., Murase, J., & Nishiuchi, S. (2022). Estimating yield-related traits using UAV-derived multispectral images to improve rice grain yield prediction. *Agriculture*, *12*(8), 1141. https://doi.org/10.3390/agriculture12081141

Chapman, S. C., Merz, T., Chan, A., Jackway, P., Hrabar, S., Dreccer, M. F., Holland, E., Zheng, B., Ling, T. J., & Jimenez-Berni, J. (2014). Pheno-copter: a low-altitude, autonomous remote-sensing robotic helicopter for high-throughput field-based phenotyping. *Agronomy*, *4*(2), 279–301. https://doi.org/10.3390/agronomy4020279

Du, L., Yang, H., Song, X., Wei, N., Yu, C., Wang, W., & Zhao, Y. (2022). Estimating leaf area index of maize using UAV-based digital imagery and machine learning methods. *Scientific Reports*, *12*, 15937. https://doi.org/10.1038/s41598-022-20299-0

Duan, B., Fang, S., Zhu, R., Wu, X., Wang, S., Gong, Y., & Peng, Y. (2019). Remote estimation of rice yield with unmanned aerial vehicle (UAV) data and spectral mixture analysis. *Frontiers in Plant Science*, *10*, 204. https://doi.org/10.3389/fpls.2019.00204

Imanni, H. S. E., Harti, A. E., & Iysaouy, L. E. (2022). Wheat yield estimation using remote sensing indices derived from sentinel-2 time series and Google Earth engine in a highly fragmented and heterogeneous agricultural region. *Agronomy*, *12*(11), 2853. https://doi.org/10.3390/agronomy12112853

Franch, B., Bautista, A. S., Fita, D., Rubio, C., Tarrazó-Serrano, D., Sánchez, A., Skakun, S., Vermote, E., Becker-Reshef, I., & Uris, A. (2021). Within-field rice yield estimation based on sentinel-2 satellite data. *Remote Sensing*, *13*(20), 4095. https://doi.org/10.3390/rs13204095

Gong, Y., Yang, K., Lin, Z., Fang, S., Wu, X., Zhu, R., & Peng, Y. (2021). Remote estimation of leaf area index (LAI) with unmanned aerial vehicle (UAV) imaging for different rice cultivars throughout the entire growing season. *Plant Methods*, *17*, 88. https://doi.org/10.1186/s13007-021-00789-4

Hazra, A. (2017). Using the confidence interval confidently. *Journal of Thoracic Disease*, *9*(10), 4125–4130. https://doi.org/10.21037/jtd.2017.09.14

Kawamura, K., Ikeura, H., Phongchanmaixay, S., & Khanthavong, P. (2018). Canopy hyperspectral sensing of paddy fields at the booting stage and PLS regression can assess grain yield. *Remote Sensing*, *10*(8), 1249. https://doi.org/10.3390/rs10081249

Li, S., Feng, Z., Yang, B., Li, H., Liao, F., Gao, Y., Liu, S., Tang, J., & Yao, Q. (2022). An intelligent monitoring system of diseases and pests on rice canopy. *Frontiers in Plant Science*, *13*, 972286. https://doi.org/10.3389/fpls.2022.972286

Lillesand, T. M., Kiefer, R. W., & Chipman, J. W. (2014). *Remote Sensing and Image Interpretation* (7th ed). John Wiley & Sons, Inc.

Muangprakhon, R., & Kaewplang, S. (2021). Estimation of paddy rice plant height using UAV remote sensing. *Engineering Access*, *7*(2), 93–97. https://doi.org/10.14456/mijet.2021.14

Munibah, K., Barus, B., Iman, L. S., Tjahjono, B., Wijayanti, R. S., Mufti, B., & Hongo, C. (2019). Utilization of sentinel-2 imagery to identify a growth phase of rice plant in Cianjur Regency, West Java, Indonesia. In Y. Setiawan et al. (Eds.), *Sixth International Symposium on LAPAN-IPB Satellite* (pp. 1–9). https://doi.org/10.1117/12.2539555

Munibah, K., Trisasongko, B. H., Barus, B., Tjahjono, B., Achmad, A., Uciningsih, W., Sigit, G., & Hongo, C. (2022). Identification of age class and varieties of rice plant using spectroradiometry and chlorophyll content index. *Majalah Ilmiah Globe*, *24*(1), 19–26.

Nazir, A., Ullah, S., Saqib, Z. A., Abbas, A., Ali, A., Iqbal, M. S., Hussain, K., Shakir, M., Shah, M., & Butt, M. U. (2021). Estimation and forecasting of rice yield using phenology-based algorithm and linear regression model on sentinel-II satellite data. *Agriculture*, *11*(10), 1026. https://doi.org/10.3390/agriculture11101026

Santosa, D. A. (2023). *Rice availability target fot 2024 is considered unreasonable.* Kompas. https://www.kompas.id/baca/ekonomi/2023/08/23/target-ketersediaan-beras-2024-dinilai-tidak-masuk-akal

Sari, M. Y. A., Hassim, Y. M. M., Hidayat, R., & Ahmad, A. (2021). Monitoring rice crop and paddy field condition using UAV RGB imagery. *International Journal on Informatics Visualization*, *5*(4), 469–474. https://doi.org/10.30630/JOIV.5.4.742

Siyal, A. A., Dempewolf, J., & Becker-Reshef, I. (2015). Rice yield estimation using Landsat ETM + Data. *Journal of Applied Remote Sensing*, *9*(1), 095986. https://doi.org/10.1117/1.jrs.9.095986

Sujarwo, Putra, A. N., Setyawan, R. A., Teixeira, H. M., & Khumairoh, U. (2022). Forecasting rice status for a food crisis early warning system based on satellite imagery and cellular automata in Malang, Indonesia. *Sustainability*, *14*(15), 8972. https://doi.org/10.3390/su14158972

Taiz, L., & Zeiger, E. (2002). *Plant physiology (3rd ed.)*. Sinauer Associates.

Wang, Y., Tan, S., Jia, X., Qi, L., Liu, S., Lu, H., Wang, C., Liu, W., Zhao, X., He, L., Chen, J., Yang, C., Wang, X., Chen, J., Qin, Y., Yu, J., & Ma, X. (2023). Estimating relative chlorophyll content in rice leaves using unmanned aerial vehicle multi-spectral images and spectral-textural analysis. *Agronomy*, *13*(6), 1541. https://doi.org/10.3390/agronomy13061541

Publisher's Note: The statements, opinions and data contained in all publications are solely those of the individual author(s) and contributor(s) and not of the publisher(s) and/or the editor(s).

Copyright: © 2024 by the authors. This article is an open access article distributed under the terms and conditions of the Creative Commons Attribution (CC BY) license (https://creativecommons.org/licenses/by/4.0/).